

# Physical model study of the wake produced by multiple cross-flow turbines

Mitchel Provan, Paul Knox, Andrew Cornett, Julien Cousineau

**Abstract**—It is well known that multiple marine energy devices will need to be placed in groups, or arrays, in order to take full advantage of the potential extractable energy of a project site. However, in order to optimize the layout of these arrays, more knowledge is required on the complex hydrodynamic interactions of devices within these arrays. The focus of this paper intends to further this research and centres on the wakes produced by multiple model cross-flow turbines, including two configurations of in-line turbines and one simple array composed of three model turbines. The wakes produced by these configurations are characterized by downstream velocity measurements and the results are presented in the form of velocity ratio (ratio of wake velocity to free-stream velocity) and turbulence intensity. The results collected from this experimental work will be used to calibrate a CFD numerical model that will be used to further investigate turbine-turbine interactions. The results from the CFD model will then help develop a hydrodynamic model that can be used as a tool to aid the development and optimization of cross-flow turbine layouts for specific project locations.

**Keywords**—cross-flow turbine, turbine array, hydrokinetic energy, physical model

## I. INTRODUCTION

TIDAL and river currents have the potential to become a viable long-term source of clean renewable energy, provided that the environmental and economic costs of producing energy from these flows can be lowered to competitive levels. In order for developers to achieve a good business return, the energy extracted at each project site needs to be maximized by deploying multiple turbines in an array. However, available information on the performance of turbines in arrays is limited and there is a need for knowledge concerning the interactions between adjacent turbines, the performance of individual turbines in arrays and the interaction of turbine arrays with the surrounding environment. This knowledge will make it possible to optimize turbine array layouts.

Scaled experimental models have previously been used to investigate the wake produced by tidal/hydrokinetic turbines. Researchers have used porous discs or plates to represent a simplified turbine in order to investigate the characteristics of turbine wakes. These discs were used to represent axial flow turbines in various placements and array configurations and the wake downstream of the porous discs was characterized in terms of velocity measurements [1][2][3]. A similar approach was employed where large turbine arrays were represented in a model through the use of simplified porous fences [4]. The drag forces acting on the fences and the velocity wake were measured. Previous studies have also characterized the downstream wake of scaled model axial-flow turbines [5][6][7]. However the wake shape and recovery rate produced by an axial-flow turbine may differ from that of a cross-flow turbine. There has been limited previous research conducted on the wakes of cross-flow turbines. In one example, the wake produced by a novel type of cross-flow turbine, the momentum-reversal-and-lift turbine was investigated through the use of scaled model turbines in different array layouts [8]. In addition, a relatively large scale (1:6) study of a vertical axis cross-flow turbine wake was carried out, however the study only focused on characterizing the near-field wake and therefore, velocity measurements were taken at only 1 turbine diameter downstream [9].

A knowledge gap currently exists regarding turbine induced wake and the wake characteristics of vertical axis cross-flow turbines, which is required knowledge in order to develop efficient array layout configurations. The primary objective of the presented research is to produce a set of guidelines that can aid developers in implementing turbine arrays. The first step of the study, and the focus of this paper, is to collect experimental data (velocity and turbulence intensity) of model cross-flow turbines that will be used in a subsequent study to help calibrate and validate a CFD model. The CFD model will be used to study turbine-turbine interactions which will then help develop a hydrodynamic model that can be used to study array-environment interactions for specific project sites.

The authors have previously completed a series of tests measuring the downstream wake of porous plates that were used to represent cross-flow turbines [10] and the wake of a single scaled cross-flow turbine as well as an in-plane turbine pair [11]. The focus of this paper will be on the wake produced by two in-line turbines at two different downstream separations and the wake of a simple array composed of three turbines.

## II. PHYSICAL MODEL

### A. Model setup

The experimental study was conducted in the Large Wave-Current Flume (LWCF) at the Ocean, Coastal and River Engineering Research Centre of the National Research Council of Canada (NRC-OCRE). The LWCF is 97m long, 2m wide and up to 2.75m deep. The facility is equipped with a current generation system that can produce flows up to  $1.1 \text{ m}^3/\text{s}$ . The water depth in the flume can be controlled and adjusted to a desired depth. For this study, the depth in the flume was maintained at 0.75m and the undisturbed flow speed in the streamwise direction ( $U_0$ ) was  $0.68 \text{ m/s}$ . A series of flow-straighteners are located upstream of the testing section to diminish any vorticity in the flow and provide a uniform uni-directional flow through the test section. An overall view of the flume is shown in Fig. 1.



Fig. 1. Overview of the LWCF.

### B. Model turbine

A scaled model of a vertical axis cross-flow turbine was designed and fabricated for this study. A sketch of the model turbine is shown in Fig. 2a and a picture of the turbine installed in the LWCF is shown in Fig. 2b. The turbine rotor was 3D printed out of nylon powder to produce a lightweight, waterproof material that can be shaped into the required airfoils with high precision. The rotor blades had a NACA63-021 profile and the support arms had a NACA-12 profile. The chord length for both

the rotor blades and the support arms was  $0.023\text{m}$  and the total diameter of the rotor was  $0.32\text{m}$ . The rotor was mounted on a  $\frac{3}{4}$ " diameter stainless steel shaft at an elevation that set the centre of the rotor at  $0.48\text{m}$  ( $1.5D$ , where  $D=0.32\text{m}$ , the rotor diameter) above the flume floor. The shaft was carefully aligned to ensure it was level and the bottom of the shaft was mounted in a marine bearing and the top of the shaft was connected to a servomotor. Both the marine bearing and servomotor were mounted to independent 6-axis load cells.

### C. Instrumentation

Two different instruments were used to measure the velocities within the flume. The upstream reference velocity was measured approximately  $25D$  upstream of the turbine by a 2-axis electromagnetic current meter (ECM) manufactured by Valeport. The downstream wake velocity was measured by five 3-axis acoustic Doppler velocimeters (ADV) manufactured by Nortek. The ADV probes were mounted to an instrumentation rack that could be moved in all three dimensions (vertically, cross-flume and along-flume) at a  $0.1\text{m}$  resolution. Thin guy-wires were used to provide additional stability to the ADV probes and reduce vibrations of the probes during testing. At each measurement location the ADV probes were sampled for  $180\text{s}$  at a sampling frequency of  $25\text{Hz}$ . This produced a total of  $4500$  "pings" at each sampling location. The ADV probes typically had a correlation percentage of  $90\%$  and a signal to noise ratio of approximately  $15\text{dB}$ .

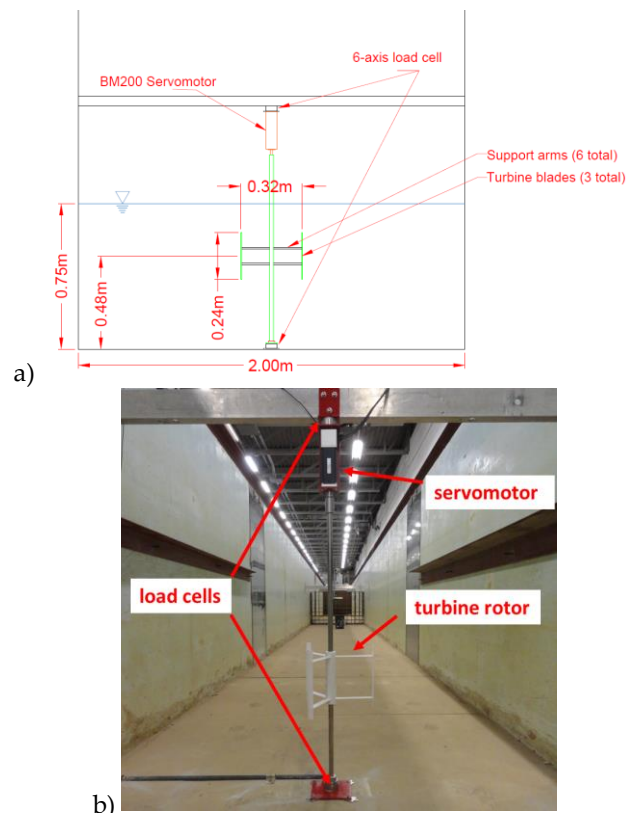


Fig. 2. a) sketch of the model cross-flow turbine and b) model turbine installed in the LWCF.

Drag forces acting on the model turbine were measured using two Mini45 IP65/IP68 load cells manufactured by ATI Industrial Automation. One load cell was attached to the top of the servomotor and the second load cell was attached underneath the marine bearing on the bottom of the flume. The hydrodynamic forces acting on the turbine rotor were isolated by measuring the drag force on only the central shaft and subtracting the measured force from the force measured on the central shaft and turbine rotor.

The servomotor, an Aerotech BM200 brushless rotary servomotor, was used to drive/brake the model turbines to match the desired tip speed ratio (TSR) for the wake characterization tests. The TSR was maintained at 2.5 throughout the testing program, which is a typical operating TSR for 3-bladed cross-flow turbines. The servomotor was able to measure and control the RPM and torque applied to the shaft.

#### D. Data Presentation

The velocity measurements acquired using the ADV probes were used to calculate two time-averaged parameters that are commonly utilized to characterize the downstream wake of turbines; the velocity ratio ( $U_{ratio}$ ) and the turbulence intensity ( $I$ ). The velocity ratio is the ratio of the wake velocity ( $U_w$ ) to the free-stream (i.e. without turbines) flow velocity ( $U_0$ ). Since the flow in the flume is primarily uni-directional in the streamwise direction ( $x$ ), the velocity ratio can be calculated using (1).

$$U_{ratio} = \frac{U_{w,x}}{U_0} \quad (1)$$

The turbulence intensity,  $I$ , relates the fluctuations in the flow ( $\sigma$ , standard deviation) to the mean flow velocity ( $\bar{u}$ ) and can be calculated for all three Cartesian directions ( $x$ ,  $y$  and  $z$ ). Similar to the velocity ratio calculation, since the flow in the flume is primarily uni-directional in the streamwise direction, the turbulence intensity reported herein is the turbulence intensity in the streamwise direction ( $I_x$ ) and is calculated using (2)

$$I_x = \frac{\sigma_x}{\bar{u}_x} \times 100\% \quad (2)$$

The force measurements,  $F_d$ , were used to calculate the drag coefficient,  $C_d$ , of the turbines using (3).

$$C_d = \frac{F_d}{0.5\rho U_0^2 A_t} \quad (3)$$

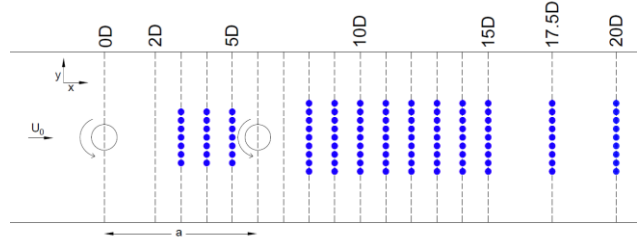
where  $\rho$  is the fluid density (998 kg/m<sup>3</sup>) and  $A_t$  is the area of the turbine rotor.

### III. MODEL RESULTS AND DISCUSSION

#### E. Testing Program

The primary goal of this study was to collect experimental data of the wake produced by vertical-axis cross-flow turbines that can be used to calibrate and validate a CFD model. The focus of this paper is on the wake produced by two in-line turbines with two different separations,  $a$  (shown in Fig. 3a) and a simple turbine array (shown in Fig. 3b).

a)



b)

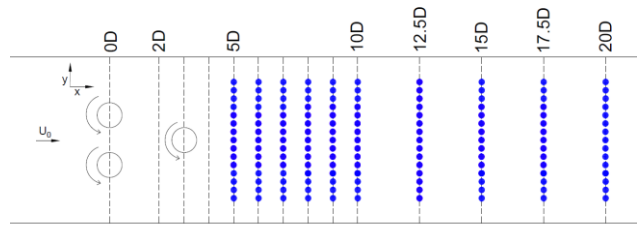


Fig. 3. Turbine arrangement and velocity measurement points (blue circles) for a) in-line turbine tests and b) array test.

For the in-line turbine configuration (Fig. 3a), velocity measurements were taken at the  $z=1.5D$  (rotor mid-height) elevation at 13 cross-sections in the space between and downstream of the two turbines. At the 3 cross-sections between the turbines, 7 individual measurements were taken along each cross-section at a  $0.33D$  spacing while 9 individual measurements were taken at the remaining cross-sections. A similar approach was taken for the simple array configuration (Fig. 3b), where 15 velocity measurements were taken at each of the 10 downstream cross-sections. This resulted in a total of 111 and 150 individual measurement locations for the in-line configuration and the simple array configuration, respectively.

#### F. Free-stream flow characteristics

Before installing the turbines in the flume, the free-stream flow velocities were measured throughout the testing section to gain an understanding of the flume's natural flow characteristics. The measurements showed a maximum of 5% variance in the flow speed throughout the testing section with an average free-stream velocity of 0.68 m/s (see Fig. 4). As shown in Fig. 4, the ambient turbulence intensity throughout the testing section was found to be 12% at the upstream end of the testing section ( $x=2D$ ) and gradually decreased to approximately 5.5% at the downstream end ( $x=20D$ ). It has been shown in previous

studies that the rate of wake recovery is influenced by the ambient turbulence intensity in the flow [6][11]. A larger ambient turbulence promotes more mixing of the wake with the surrounding flow compared to a lower ambient turbulence. Therefore, the rate of wake recovery in this study can be expected to decrease with downstream distance. This may result in a wake that would be longer than what would occur if the ambient turbulence intensity was maintained throughout the entire testing section.

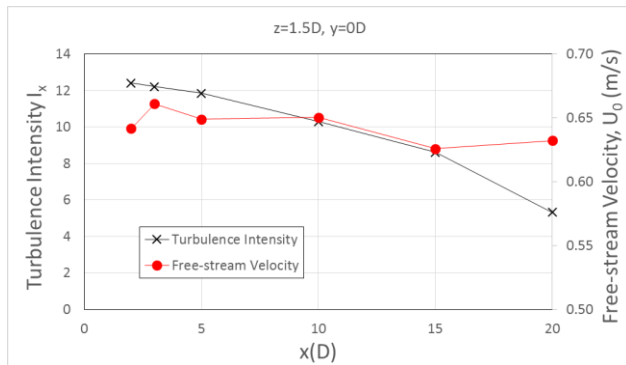


Fig. 4. Measured free-stream turbulence intensity and velocity within the testing section.

#### G. In-line turbines separated by $a=6D$

Two turbines were installed along  $y=0D$  (centre of the flume); an upstream turbine at  $x=0D$  (herein referred to as the “first turbine”) and a downstream turbine at  $x=6D$  (herein referred to as the “second turbine”), producing a longitudinal spacing of  $a=6D$  between the two turbines. Velocity measurements were taken in the space between and downstream of the two turbines and the resulting velocity ratio,  $U_{w,x}/U_0$ , and turbulence intensity,  $I_x$ , are provided in Fig. 5. The flow velocity immediately upstream of the second turbine shows that the wake produced by the first turbine has recovered to 57% of the free-stream velocity before reaching the downstream turbine. Downstream of the second turbine ( $x=8D$ ), the flow velocity drops to 14% of the free-stream velocity and then rapidly recovers as the wake progresses downstream, reaching 60% of the free-stream velocity by  $x=10D$ . Downstream of approximately  $x=12D$ , the rate of wake recovery slows down and by the end of the testing section ( $x=20D$ ) the wake recovers to 88% of the free-stream velocity. These results are compared against the results of a single turbine installed at  $x=0D$  with no downstream turbine [11], which are also plotted in Fig. 5. The wake between the two in-line turbines recovers slower compared to that of the single turbine. This could be due to the downstream turbine creating an increase in hydraulic head upstream of the turbine, thereby reducing the flow velocity compared to the same location downstream of the single turbine. The wake produced by the in-line configuration and the wake produced by a single turbine show a similar rate of recovery downstream of  $x=15D$ . However, the wake velocity of the in-line configuration is lower compared to that of the single turbine. The wake of the single turbine reaches 90% of the

free-stream velocity by  $x=14D$ , while the wake of the in-line turbines recovered to 88% by  $x=20D$ , which is the downstream limit of the testing section. A similar trend between the in-line configuration and the single turbine was seen in the turbulence intensity measurements. Between  $x=3D$  and  $x=5D$  the in-line turbine wake and the single turbine wake had similar turbulence intensities. Downstream of the second turbine, the turbulence intensity peaked at 80% at  $x=8D$  and decreased to 15% by  $x=20D$ . The single turbine had a turbulence intensity of 9% at  $x=20D$ , 6% lower than the in-line configuration. Overall, adding a second turbine at  $6D$  downstream of the first turbine shows a similar, albeit smaller, wake recovery compared to that of a single turbine. The far-field wake of the in-line turbines is approximately 8% lower compared to the scenario with only a single turbine.

The drag force acting on each turbine was measured and the drag coefficients were calculated to be 0.71 for the first turbine and 0.48 for the second turbine. A reduced hydrodynamic force acting on the downstream turbine is expected as the wake of the upstream turbine reduces the in-flow velocity for the downstream turbine.

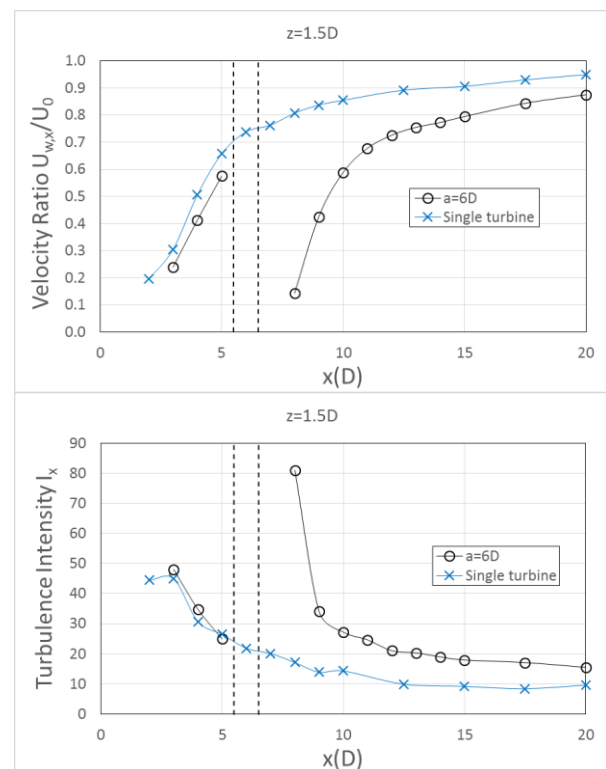


Fig. 5. Longitudinal variation of velocity ratio and turbulence intensity at  $y=0D$  (centreline of the turbines) for two in-line turbines separated by  $a=6D$  (black circles) and a single turbine (blue 'x's). Dashed lines indicate diameter of downstream turbine.

#### H. In-line turbines separated by $a=12D$

Following the mapping of the in-line turbine wake produced by a turbine separation of  $6D$ , the first turbine previously located at  $x=0D$  was moved  $6D$  upstream to increase the total distance between the two in-line turbines to  $12D$ .

Similar to the previous configuration, velocity measurements were taken in the space between and



downstream of the two turbines. The resulting velocity ratio and turbulence intensity plots are provided in Fig. 6 and are plotted against the results of the 6D separation. The increased distance between the two turbines produces a significant impact on the velocities between the turbines. The larger turbine spacing produces a higher velocity ratio between  $x=3D$  and  $x=5D$  compared to the smaller turbine spacing. This can be expected as the larger turbine separation provides a longer distance for the wake of the first turbine to recover compared to the smaller 6D separation. These higher flow velocities present in the 12D separation increased the performance of the second turbine by approximately 15% compared to the 6D separation. This is reflected in the drag force measurements where the drag coefficient for the second turbine increased from 0.48 to 0.58 due to the increase in separation distance from 6D to 12D. A similar trend is seen in the turbulence intensity results where the 6D separation produces a higher turbulence intensity at  $x=5D$  compared to the 12D separation (25% compared to 5%).

Downstream of  $x=6D$  (location of the second turbine in both in-line configurations), the wakes produced by both in-line configurations show similar velocity ratios and turbulence intensities. Both wake velocities recover to approximately 87% by  $x=20D$ . This indicates that the wake recovery downstream of the second turbine is independent of the proximity of the first turbine for the tested separation distances of 6D-12D.

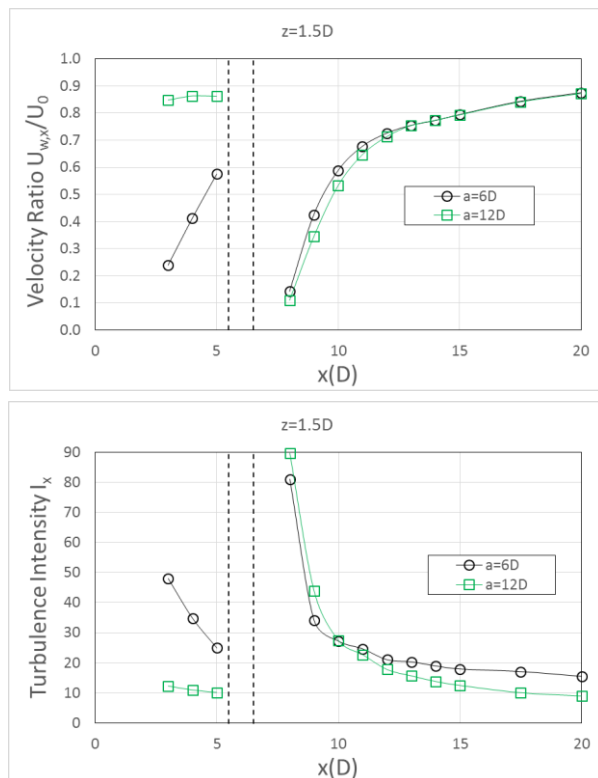


Fig. 6. Longitudinal variation of velocity ratio and turbulence intensity at  $y=0D$  for two in-line turbine separations;  $a=6D$  (black circles) and  $a=12D$  (green squares). Dashed lines indicate diameter of downstream turbine (upstream turbine located at  $-6D$  not shown).

The plots in Fig. 7 show the lateral variation (along the  $y$ -axis) of velocity ratio for both in-line turbine separations; 6D and 12D. In Fig. 7 the rotor blades are moving upstream near the upper dashed horizontal line and moving downstream near the lower dashed horizontal line. The measured data reveals that the wakes of both separation distances are slightly asymmetric in the horizontal plane, with the velocity ratio being lower toward the up-blade side of the turbine (upper dashed line). This suggests that the turbine blade moving upstream against the incident flow creates a large velocity deficit compared to the opposite side of the turbine where the blade moves in the same direction as the incident flow. At  $x=3D$ , there is a clear discrepancy of the wake between the two turbines for each separation distance. The wake recovery of the 12D separation has progressed further and is a more uniform wake compared to that of the 6D separation. The results also show that the velocity ratio between the turbine edge and the flume wall is accelerated compared to the free-stream velocity ( $U_{w,x}/U_0 > 1$ ). This is a product of the blockage effect of the turbines where the flow is accelerated around the edge of the turbines. This blockage effect appears to be relatively unaffected by the separation distance between the two in-line configurations. Further downstream of the second turbine the lateral velocity profiles of both in-line configurations are more similar across the width of the measured points. This reinforces the conclusion that the wake downstream of the second turbine is relatively unaffected by the proximity of the upstream turbine. At  $20D$  downstream, the wakes for both separation distances are more uniform as the wakes continue to mix and merge with the surrounding flow.

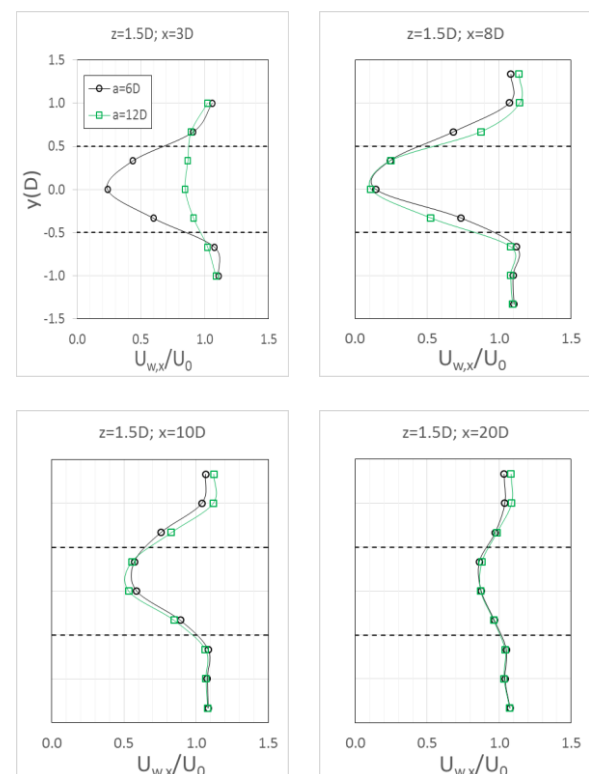


Fig. 7. Lateral variation of velocity ratio at different downstream locations for two in-line turbine separations;  $a=6D$  (black circles) and  $a=12D$  (green squares). Dashed lines indicate diameter of turbine.

### I. Simple turbine array

A simple turbine array was installed in the flume (see Fig. 3b) with two upstream turbines (herein referred to as the “first row turbines”) installed at  $x=0D$  with a  $1D$  separation between the two turbines. This placed one turbine centre at  $y=-1D$  and one turbine centre at  $y=1D$ . A third turbine (herein referred to as the “second row turbine”) was installed downstream at  $x=3D$  and was centred within the gap between the first row turbines ( $y=0D$ ). Velocity measurements were taken downstream of the turbine array starting at  $x=5D$ . Velocity measurements were not able to be taken in between the two rows of turbines due to the close proximity of the turbines. The results of the velocity measurements are shown in Fig. 8 for two  $y$ -locations;  $y=0D$  (gap centreline between the first row turbines/along the centreline of the second row turbine) and at  $y=1D$  (centreline of one of the first row turbines). The two longitudinal profiles show a large difference between wakes emanating from the two turbines. The wake along  $y=0D$  shows a similar profile to the wake of a single turbine (see single turbine results in Fig. 5). The velocity ratio is 32% of the free-stream velocity at  $x=5D$  (2D downstream of the second row turbine) and recovers to 90% of the free-stream velocity by approximately  $x=19D$ . The velocity ratio results along  $y=1D$  shows a very different result compared to the single turbine scenario. The wake velocities have already recovered to 83% of the free-stream velocity by  $x=5D$  and the wake remains largely unchanged until  $x=12.5D$ , where it then begins to recover at a similar rate as the wake along  $y=0D$ . This quick recovery of the first row turbine wake may be attributed to increased mixing due to the presence of the second row turbine. Previous work [11] has shown that a high velocity jet forms between a turbine pair (with no downstream turbine present) and the wake recovery of each individual turbine within the pair is similar to the wake recovery of a single turbine. However, it is evident that introducing the second row turbine within this high velocity jet (in the case of this study, along  $y=0D$ ) has a significant effect on the wake of the two upstream turbines. The blockage effect of a single turbine, as discussed in the results of the in-line turbines, will accelerate flow around the edges of the turbine. Therefore, the array’s second row turbine produces a flow blockage that directs flow around the edges of the turbine and this redirected flow mixes with the wake of the first row turbines; increasing the wake recovery of the first row turbines.

The plots in Fig. 9 show the lateral variation (along the  $y$ -axis) of the velocity ratio for the simple array configuration. The individual wakes of the three turbines are clearly identifiable at  $x=5D$ , with the second row turbine producing a more severe wake compared to the

first row turbines. Once the wakes reach  $x=8D$  they begin to merge into one larger wake that is more uniform across the width of the array. Further downstream, at  $x=10D$ , the individual wakes are almost indistinguishable and as the single large wake continues downstream it recovers to approximately 90% of the free-stream velocity once it reaches  $x=20D$ . It can be extrapolated from Fig. 8 that downstream of  $x=20D$ , the rate of wake recovery would be quite slow and may take much further downstream until the wake is fully recovered to the free-stream conditions ( $U_{w,x}/U_0=1$ ). Therefore,  $20D$  downstream of the first row of the array presents a reasonable location for the next row of the array to be installed.

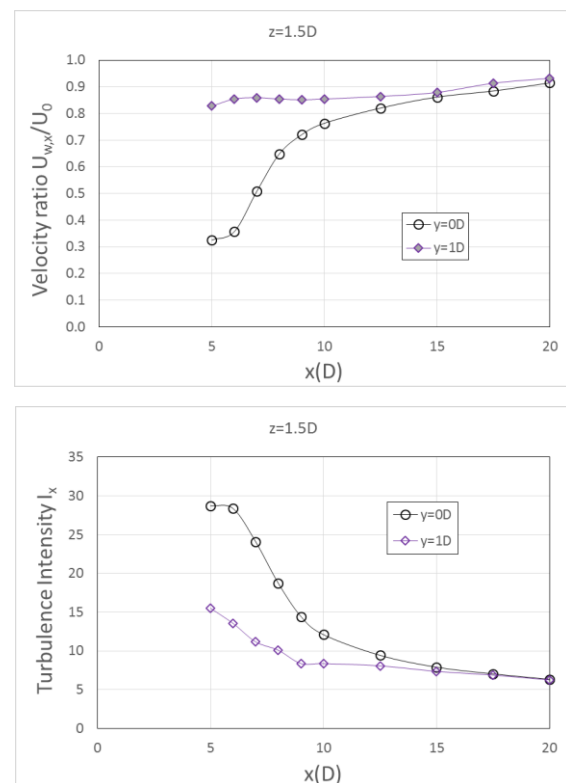


Fig. 8. Longitudinal variation of velocity ratio and turbulence intensity at  $y=0D$  (black circles) and  $y=1D$  (purple diamonds) for the simple array configuration.

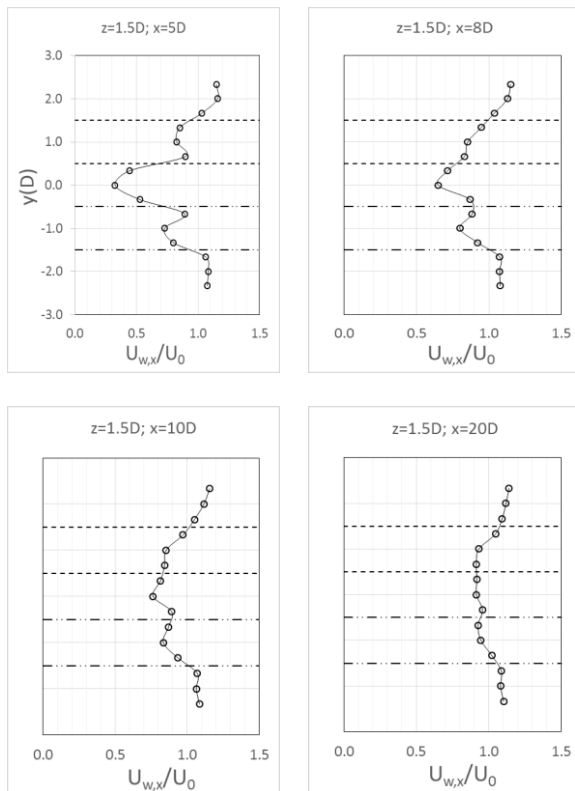


Fig. 9. Lateral variation of velocity ratio at different downstream locations for the simple array configuration. Dashed lines indicate diameter of upstream turbines.

#### IV. CONCLUSION

The wake velocities of two in-line model vertical cross-flow turbines were measured for two different configurations; a 6D spacing and a 12D spacing. When compared to the results of a single upstream turbine, it was found that introducing a second turbine 6D downstream produces a wake that recovers at a similar rate to the single turbine scenario, just delaying that recovery further downstream. Increasing the spacing between the two turbines to 12D had little effect on the downstream wake, with both in-line turbine separations producing almost identical downstream wakes. There was however a difference in the wake in-between the two turbines. The 6D turbine separation produced approximately 30% lower velocities immediately upstream of the second turbine compared to the 12D separation. Therefore, while the downstream wakes of the two configurations are similar, the larger separation distance will provide higher inflow velocities for the downstream turbine, and therefore increased turbine performance (by approximately 15%) compared to the 6D spacing.

A similar exercise was completed for a simple turbine array of three model turbines. Two turbines were placed with a 1D gap separating the upstream turbines and a third turbine was placed within the gap, 3D downstream. The presence of the second row turbine increased the wake recovery of the first row turbines when compared to the result of a single turbine. This was due to the second row turbine causing a flow blockage and directing flow around the edges of the turbine and thereby mixing with the

wakes emanating from the first row turbines. Starting at approximately 8D downstream, the individual turbine wakes began to merge into one larger wake as the wakes progressed downstream. By 20D downstream this large wake managed to recover to 90% of the free-stream velocities, providing a reasonable location for the next turbine row of an array.

The results of these configurations will be used to help calibrate and validate a CFD model which will be used to investigate additional turbine-turbine interactions. The goal of the CFD model is to develop the capability to implement the energy extraction of turbine arrays into a hydrodynamic model which can be used to help optimize cross-flow turbine arrays for specific project sites.

#### ACKNOWLEDGEMENT

The authors would like to thank Natural Resources Canada and the National Research Council of Canada for funding this study.

#### REFERENCES

- [1] L.E. Myers and A.S. Bahaj, "Experimental analysis of the flow field around horizontal axis tidal turbines by used of scale mesh disk rotor simulators," *Ocean Engineering*, vol. 37, pp. 218-227, 2010.
- [2] L.E. Myers, B. Keogh and A.S. Bahaj, "Experimental investigation of inter-array wake properties in early tidal turbine arrays," *Oceans '11 MTS*, Waikola, USA, 2011.
- [3] L.E. Myers and A.S. Bahaj, "An experimental investigation simulating flow effects in first generation marine current energy converter arrays," *Renewable Energy*, vol. 37, pp. 28-36, 2012.
- [4] D.S. Coles, L.S. Blunden, and A.S. Bahaj, "Experimental validation of the distributed drag method for simulating large marine current turbine arrays using porous fences," *International Journal of Marine Energy*, vol. 16, pp. 298-316, 2016.
- [5] T. Stallard, R. Collings, T. Feng and J. Whelan, "Interactions between tidal turbine wakes: experimental study of a group of three-bladed rotors," *Phil Trans R Soc A*, vol. 371, 2013.
- [6] P. Mycek, B. Gaurier, G. Germain, G. Pinon and R. Rivoalen, "Numerical and experimental study of the interaction between two marine current turbines," *International Journal of Marine Energy*, Vol. 1, pp. 70-83, 2013.
- [7] P. Mycek, B. Gaurier, G. Germain, G. Pinon and R. Rivoalen, "Experimental study of the turbulence intensity effects on marine current turbines behaviour. Part II: Two interacting turbines," *Renewable Energy*, Vol. 68, pp. 876-892, 2014.
- [8] S. Ordonez-Sanchez, D. Sutherland, G. Payne, T. Bruce, M. Gebreslassie, M. Belmont and I. Moon, "Experimental evaluation of the wake characteristics of cross flow turbine arrays," *Ocean Engineering*, vol. 141, pp. 215-226, 2017.
- [9] P. Bachant and M. Wosnik, "Characterizing the near-wake of a cross-flow turbine," *Journal of Turbulence*, vol. 16, pp. 392-410, 2015.
- [10] P. Knox, M. Provan, A. Cornett, E. Murphy and J. Cousineau, "Experimental study of velocity deficit and wake due to single and multiple rectangular porous plates in steady flow," *Coastlab18*, Santander, Spain, 2018.
- [11] M. Provan, A. Cornett, P. Knox, J. Cousineau and S. Ferguson, "Experimental study of the wake produced by single and multiple cross-flow turbines," *Journal of Ocean Technology*, currently submitted for publication.